

# Vaporization of Protic Ionic Liquids Studied by Matrix-Isolation Fourier Transform Infrared Spectroscopy

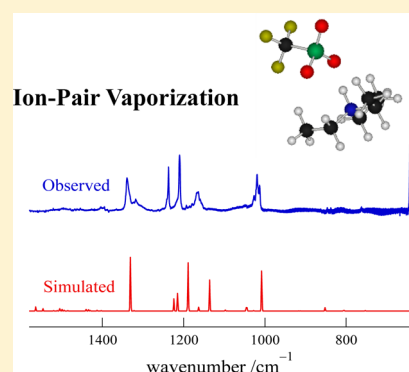
Mami Horikawa,<sup>‡</sup> Nobuyuki Akai,<sup>\*,†</sup> Akio Kawai,<sup>‡</sup> and Kazuhiko Shibuya<sup>‡</sup>

<sup>†</sup>Graduate School of Bio-Applications and Systems Engineering (BASE), Tokyo University of Agriculture and Technology, 2-24-16, Naka-cho, Koganei, Tokyo, 184-8588, Japan

<sup>‡</sup>Department of Chemistry, Graduate School of Science and Engineering, Tokyo Institute of Technology, 2-12-1, Ohokayama, Meguro-ku, Tokyo, 152-8551 Japan

## S Supporting Information

**ABSTRACT:** Several protic ionic liquids (PILs) with a wide range of  $pK_a$  differences ( $\Delta pK_a$ ) between the parent acid and base molecules were thermally evaporated in vacuum, trapped on a CsI plate by a cryogenic neon matrix-isolation method, and studied by Fourier transform infrared spectroscopy and density functional theory calculations. The parent neutral molecules and proton-transferred cation–anion pair species were identified as chemical components evaporated from the PILs with lower and higher  $\Delta pK_a$  values, respectively. The  $\Delta pK_a$ -dependent vaporization mechanism is discussed in terms of thermodynamic equilibrium between acid–base and anion–cation systems in the liquid phase.



## INTRODUCTION

Ionic liquids (ILs) made of anions and cations have unique physicochemical properties different from those of ordinal molecular liquids and have received extensive attention from researchers in a wide range of fields from basic science to many practical applications. For a long time, nonvolatility had been believed to be distinctive property of ILs, but some evaporable aprotic ILs were discovered by Earle et al. in 2006.<sup>1</sup> After the landmark report on the evaporation, gaseous chemical components evaporated from ILs have been investigated cooperatively by spectroscopic experimentalists<sup>2–15</sup> and theoreticians.<sup>14–19</sup> Nowadays, one generally accepts a vaporization mechanism in which the chemical components thermally evaporated from aprotic ILs are of cation–anion pairs and electrically neutral as a whole. The vaporization enthalpies of many aprotic ILs have been reported,<sup>20–22</sup> and recently some aprotic ILs have been found to be vaporized as gaseous chemical species made of one dication and two anions.<sup>23–25</sup>

On the other hand, the vaporization processes of protic ionic liquids (PILs) have not been understood well. PILs are prepared by proton transfer reactions from Brønsted acid (HA) to Brønsted base (B):  $HA + B \rightarrow A^- + H-B^+$ . In this paper,  $[H-B][A]$  denotes PIL in the liquid phase, and the gaseous chemical species evaporated from  $[H-B][A]$  are described by “ion-pair” and/or “parent molecules” for the cases of  $A^-H-B^+$  and  $HA + B$ , respectively. Leal et al. reported Fourier transform ion cyclotron resonance mass spectrometry (FT-ICR-MS) of the gaseous component evaporated from 1-methylimidazolium ethanoate,  $[H-MIM][AcO]$ , and concluded the evaporated species to be “parent molecules”, that is, two

independent molecules of acetic acid and methylimidazole.<sup>3</sup> The identification of the two parent molecules was also confirmed using Raman spectroscopy by Berg et al.<sup>26</sup> They reported on the results of 1,1,3,3-tetramethylguanidinium chloride and bromide, or  $[H-TMG][Cl]$  and  $[H-TMG][Br]$ , and concluded that “ion pairs” probably do not exist in the gaseous species,<sup>27,28</sup> which accords with the results of the FT-ICR-MS study.<sup>28,29</sup> A theoretical work on 1-methylimidazolium nitrate,  $[H-MIM][NO_3]$ , also predicts that the PIL vaporizes as two “parent molecules”, methylimidazole and  $HNO_3$ .<sup>30</sup> As pointed out by previous reports,<sup>31,32</sup> the vaporization mechanism of PILs would depend on the ionicity related with the acidity and basicity of parent molecules. The ionicity is estimated by using a difference in the aqueous  $pK_a$  of the acid (HA) and the protonated base ( $H-B^+$ ), which is defined as  $\Delta pK_a = pK_a(H-B^+) - pK_a(HA)$ . Although the  $pK_a$  difference ( $\Delta pK_a$ ) is derived from  $pK_a$  determined in aqueous systems, clear correlations between  $\Delta pK_a$  and physicochemical properties of pure PILs, like viscosity and ionic conductivity, are well-known.<sup>33–35</sup>

In the present study, we focused on the relationship between  $\Delta pK_a$  and chemical species vaporized from PILs, where nine PILs were synthesized from different combinations of three acids and three bases. The chemical components vaporized from each PIL were identified by matrix-isolation IR spectroscopy.

Received: February 19, 2014

Revised: April 8, 2014

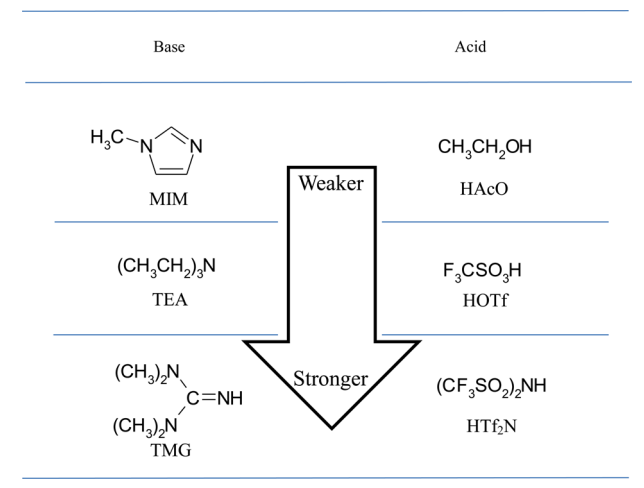
Published: April 11, 2014

copy aided by quantum chemical calculations by reference to our previous studies of aprotic ILs.<sup>8,12</sup>

## EXPERIMENTAL METHODS

**Materials.** All PILs were synthesized by mixing equimolar quantities of acid and base molecules. Three parent bases and acids employed are shown in Scheme 1. Parent acids of acetic

**Scheme 1. Parent Base and Acid Molecules Employed for the Synthesis of PILs**



acid (HAcO), bis(trifluoromethanesulfonyl)amide (HTf<sub>2</sub>N) and trifluoromethylsulfoate (HOTf), were obtained from Kanto Chemical. The three parent bases were 1-methylimidazole (MIM, from Acros Organics), triethylamine (TEA, from Wako Pure Chemical Industries), and 1,1,3,3-tetramethylguanidine (TMG, from Tokyo Chemical Industry) and were used without further purification. The PILs were synthesized on a Teflon-coated stainless-steel heating unit and purified in a vacuum chamber under  $<10^{-5}$  Pa for more than 1–10 h to remove excess parent molecule (acid or base) and impurity water. The synthesized PILs are listed in Table 1, together with their  $\Delta pK_a$  values.

**Matrix-Isolation FTIR Spectra.** The purified sample was moderately evaporated and mixed with much excess neon gas in the heating unit attached on the head of a deposition nozzle. Each gaseous parent molecule was premixed with 1000-fold

**Table 1. Gaseous Components Evacuated from Synthesized Protic ILs with  $\Delta pK_a$  Values of Parent Acid and Base Molecules**

protic ionic liquid	$\Delta pK_a^a$	vaporized components	vaporization temperature (K)
[H-MIM][AcO]	2.6	parent molecules	298
[H-TEA][AcO]	5.8	parent molecules	298
[H-Tmg][AcO]	8.8	not detected <sup>b</sup>	
[H-Mim][Otf]	14.4	not detected <sup>b</sup>	
[H-Tea][Otf]	17.6	ion-pair	363
[H-Tmg][Otf]	20.6	not detected <sup>b</sup>	
[H-Mim][Tf <sub>2</sub> N]	17.4	parent molecules	393
[H-TEA][Tf <sub>2</sub> N]	20.6	ion-pair <sup>c</sup>	388
[H-TMG][Tf <sub>2</sub> N]	23.6	ion-pair	428

<sup>a</sup>The values determined in aqueous solutions are obtained from refs 31 and 35. <sup>b</sup>See text. <sup>c</sup>A trace of the corresponding acid was additionally detected for the vaporization at 433 K. See text.

neon gas in a glass reservoir at room temperature. The gas mixture was deposited on a CsI plate cooled to ca. 6 K by a closed-cycle helium refrigerator (Iwatani, Cryo Mini). The matrix-isolated sample was measured with an FTIR spectrophotometer (JEOL, SPX200ST) equipped with an MCT detector (spectral resolution,  $0.5\text{ cm}^{-1}$ ; accumulation number, 100). The IR spectra of neat PILs were obtained with  $4\text{ cm}^{-1}$  resolution by an ATR method using a ZnSe crystal or a transmission of the sample sandwiched between two KBr plates.

**Quantum Chemical Calculation.** The energies, geometries, and vibrational spectra of PILs and their parent molecules were calculated by a density functional theory (DFT) method on the Gaussian09 program package.<sup>36</sup> The B3LYP as a typical hybrid-functional of DFT was used with a basis set of 6-311++G(3df,3pd). All calculations were executed by a TSUBAME supercomputer of Tokyo Institute of Technology.

## RESULTS AND DISCUSSION

**Protic ILs Synthesized from HAcO Acid.** Figure 1 shows the IR spectra relevant to a PIL of [H-MIM][AcO], which was

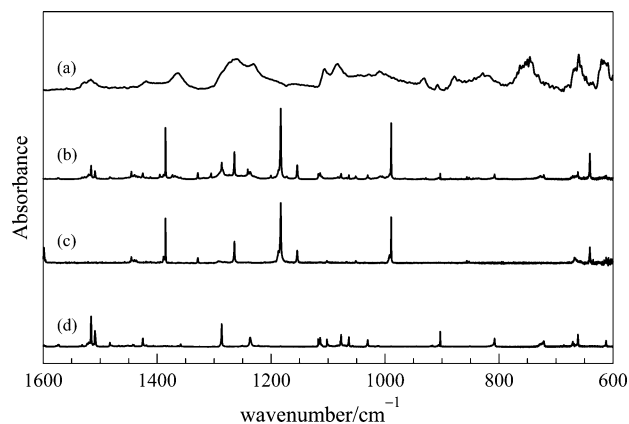


**Figure 1.** IR spectra of [H-MIM][AcO]. Spectrum a was measured for neat [H-MIM][AcO] liquid at room temperature. Spectra b, c, and d were recorded for the cryogenic neon matrix-isolated samples of gaseous components evaporated from [H-MIM][AcO], HAcO, and MIM, respectively.

synthesized by a combination of HAcO and MIM (the weakest acid and base molecules, respectively, listed in Scheme 1). The IR spectrum of neat [H-MIM][AcO] liquid measured at room temperature is shown in Figure 1a. Figure 1b shows the matrix isolation spectrum of chemical components vaporized at room temperature from neat [H-MIM][AcO] liquid, which is apparently different from that of the neat PIL spectrum. The spectrum of Figure 1c,d, which correspond to the matrix-isolation spectra of two authentic chemical species, HAcO and MIM, respectively. This observation means that the parent Brønsted acid and base molecules vaporize from neat [H-MIM][AcO] liquid, which agrees with previous reports.<sup>25,26</sup>

Similar experimental results were obtained for the IR spectra relevant to the other PIL of [H-TEA][AcO] shown in Figure 2. The matrix-isolation spectrum of [H-TEA][AcO] (Figure 2b) is different from the IR spectrum of neat [H-MIM][AcO] liquid (Figure 2a) and also accords with the superposition of

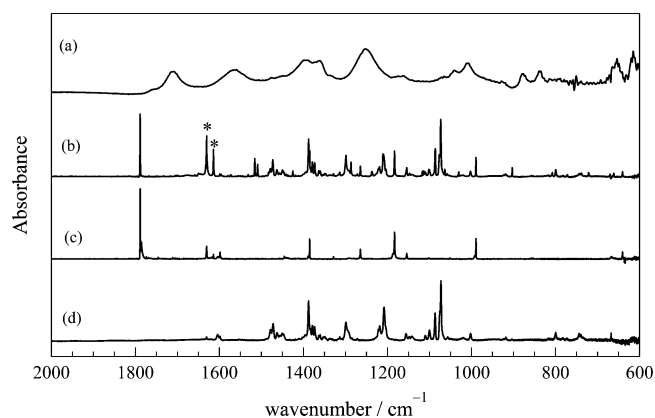


**Figure 2.** IR spectra of [H-TEA][AcO]. Spectrum a was measured for neat [H-TEA][AcO] liquid at room temperature. Spectra b, c, and d were recorded for the cryogenic neon matrix-isolated samples of gaseous components evaporated from [H-TEA][AcO], HAcO, and TEA, respectively. The bands marked with an asterisk were assigned to impurity water, which was hardly removed from samples through a standard evacuation procedure in vacuum.

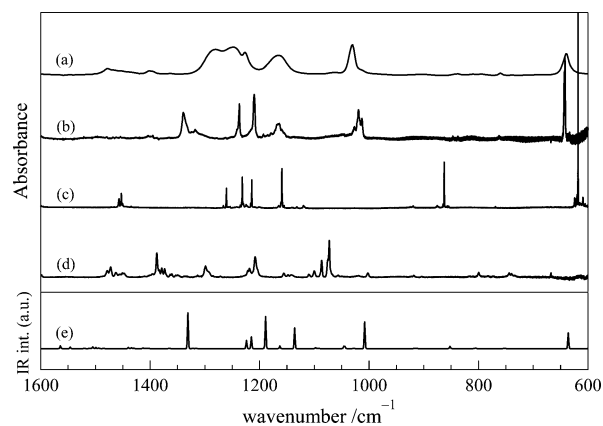


**Figure 3.** IR spectra of [H-TEA][OTf]. Spectrum a was measured for neat [H-TEA][OTf] liquid at room temperature. Spectra b, c, and d were recorded for the cryogenic neon matrix-isolated samples of gaseous components evaporated from [H-TEA][OTf], HOTf, and TEA, respectively. Spectrum e was simulated for the most stable ion-pair structure shown in Figure 7.

the matrix-isolation spectra of HAcO and TEA (spectra c and d of Figure 2, respectively).

We could not measure the matrix-isolation spectrum of [H-TMG][AcO] in the present study because the vapor pressure of [H-TMG][AcO] on the heating unit at room temperature was too high for preparing the matrix-isolated sample. This indicates that the parent TMG and HAcO molecules vaporize from [H-TMG][AcO] at room temperature.

**Protic ILs Synthesized from HOTf Acid.** Spectra a and b of Figure 3 show the IR spectra of neat [H-TEA][OTf] liquid and the matrix-isolated gaseous sample, respectively. In contrast to the results observed for protic ILs synthesized from HAcO acid, the matrix spectrum (Figure 3b) seems to be more similar to the neat spectrum (Figure 3a), but quite different from the superposition of two matrix-isolation IR spectra of the parent acid and base molecules (spectra c and d of Figure 3, respectively). The IR bands due to parent HOTf and TEA are hardly recognized in Figure 3b. For example, the 857 and 1073  $\text{cm}^{-1}$  bands characteristic of HOTf and TEA, respectively, are

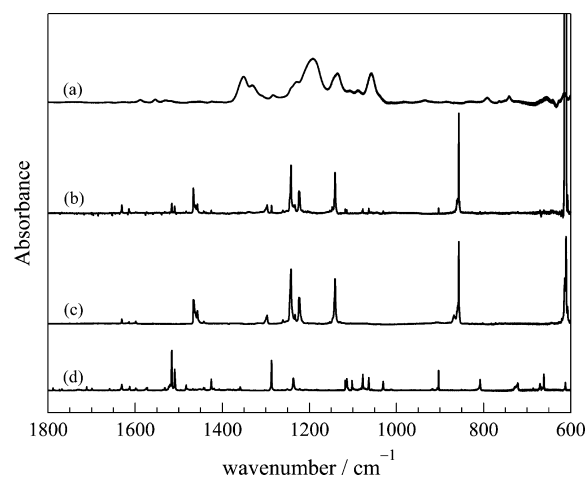


**Figure 4.** IR spectra of [H-MIM][Tf<sub>2</sub>N]. Spectrum a was measured for neat [H-MIM][Tf<sub>2</sub>N] liquid at room temperature. Spectra b, c, and d were recorded for the cryogenic neon matrix-isolated samples of gaseous components evaporated from [H-MIM][Tf<sub>2</sub>N], HTf<sub>2</sub>N, and MIM, respectively. The synthesized [H-MIM][Tf<sub>2</sub>N] sample has negligible vapor pressure at room temperature and was evaporated at 393 K.

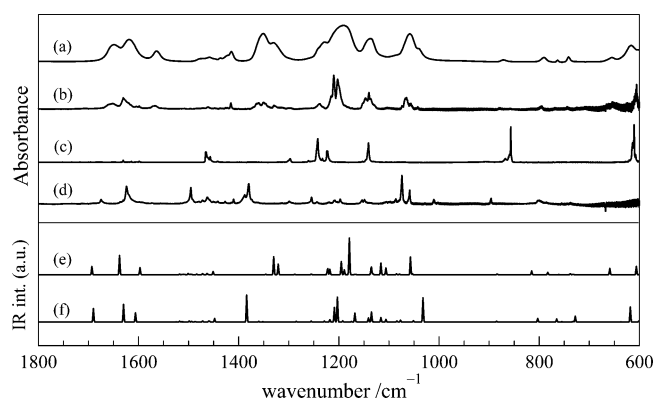


**Figure 5.** IR spectra of [H-TMG][Tf<sub>2</sub>N]. Spectrum a was measured for neat [H-TMG][Tf<sub>2</sub>N] liquid at room temperature. Spectra b, c, and d were recorded for the cryogenic neon matrix-isolated samples of gaseous components evaporated from [H-TMG][Tf<sub>2</sub>N], HTf<sub>2</sub>N, and TMG, respectively. The synthesized [H-TMG][Tf<sub>2</sub>N] sample has negligible vapor pressure at room temperature, and was evaporated at 428 K. Spectra e and f were simulated for structure A and structure B, respectively, shown in Figure 8.

not recognized in Figure 3b, which means that both the parent molecules do not exist in the vapor evaporated from neat [H-TEA][OTf] liquid. Additionally, the bandwidths of peaks in Figure 3b are broader than those observed in Figures 1b and 2b, which suggests that molecular complexes like ion pairs are isolated in the cryogenic matrix. The broad spectral feature was also recognized in other matrix-isolation spectra of evaporable aprotic ILs, where the gas phase formation of ion pairs was confirmed by matrix isolation spectroscopy of the deposited vapor.<sup>8,12</sup> Therefore, we tentatively conclude that liquid [H-TEA][OTf] vaporizes as not the parent acid and base molecules but the proton-transferred ion-pair complex. We will discuss this point later by considering remarkable differences of the neat and matrix-isolation spectra aided by quantum chemical calculations, especially in the 1100–1400  $\text{cm}^{-1}$  region.

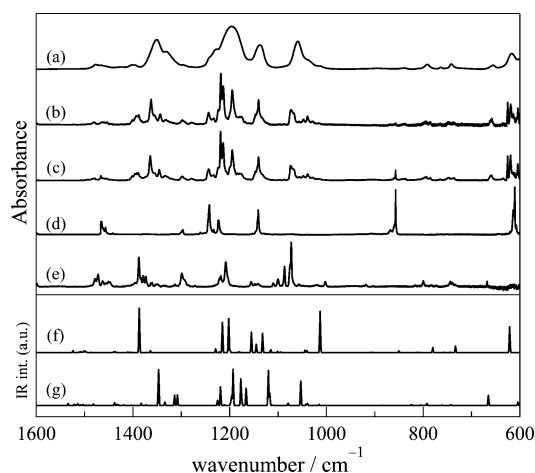


**Figure 6.** IR spectra of [H-TEA][Tf<sub>2</sub>N]. Spectrum a was measured for neat [H-TEA][Tf<sub>2</sub>N] liquid at room temperature. Spectra b and c were recorded for the cryogenic neon matrix-isolated samples of gaseous components evaporated from [H-TEA][Tf<sub>2</sub>N] at 388 and 433 K, respectively. Spectra d and e correspond to the matrix-isolation spectra of authentic samples of HTf<sub>2</sub>N and TEA. Spectra f and g were simulated for structure C and structure D, respectively, shown in Figure 9.

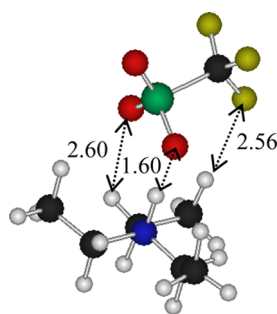


**Figure 7.** Most stable ion-pair structure of [H-TEA][OTf] calculated at the B3LYP/6-311++G(3df,3pd) level. The hydrogen bonds are indicated by the distances in angstroms.

We also synthesized two acid–base combinations of [H-MIM][OTf] and [H-TMG][OTf]. However, neat [H-MIM][OTf] existed as a solid at room temperature and thermally decomposed without vaporization. Though we could not vaporize neat [H-TMG][OTf] by heat, Zhu et al. successfully vaporized the sample by injecting a chloroform solution of [H-TMG][OTf] into a conventional GC/MS apparatus and concluded that the gaseous components are composed of the parent molecules and ionic aggregates.<sup>31</sup>

**Protic ILs Synthesized from HTf<sub>2</sub>N Acid.** Figures 4, 5, and 6 show the IR spectra relevant to three synthesized PILs of [H-MIM][Tf<sub>2</sub>N], [H-TMG][Tf<sub>2</sub>N], and [H-TEA][Tf<sub>2</sub>N], respectively. The matrix-isolation spectrum of [H-MIM][Tf<sub>2</sub>N] (Figure 4b) is quite different from that of neat [H-MIM][Tf<sub>2</sub>N] (Figure 4a) and corresponds with the superposition of two matrix-isolation IR spectra of the parent acid and base molecules shown in spectra c and d of Figure 4, respectively.

On the other hand, the matrix-isolation spectra of [H-TMG][Tf<sub>2</sub>N] (Figure 5b) and [H-TEA][Tf<sub>2</sub>N] (Figure 6b) are similar to those of the corresponding neat PILs of [H-TMG][Tf<sub>2</sub>N] (Figure 5a) and [H-TEA][Tf<sub>2</sub>N] (Figure 6a), respectively. The superposition of two matrix-isolation IR

**Table 2.** Observed and Calculated Wavenumbers of Neat [H-TEA][OTf] Liquid with Band Assignments

obs.		calc. <sup>b</sup>		
$\bar{\nu}$ (cm <sup>-1</sup> )	abs.	$\bar{\nu}$ (cm <sup>-1</sup> )	int. (km mol <sup>-1</sup> )	assignment
1404	9.1			
1395	6.4			
1339	59.3	1331	100	$\nu(\text{SO}_3)$
1318	20.3			
1241	20.2	1224	22.9	$\nu(\text{CF}_3) + \nu(\text{SO}_3)$
1237	78.0	1215	32.8	$\nu(\text{CF}_3) + \nu(\text{SO}_3)$
1210	100	1189	89.5	$\nu(\text{CF}_3) + \nu(\text{SO}_3)$
1193	9.7	1163	7.21	$\nu(\text{CF}_3) + \nu(\text{SO}_3)$
1180	12.1			
1164	33.8	1136	57.9	$\nu(\text{CF}_3)$
1159	20.7			
1026	26.4	1046	6.1	$\nu(\text{NCC})$
		1044	6.0	$\nu(\text{NCC})$
1019	64.4	1008	74.4	$\nu_s(\text{SO}_3)$
1013	45.3			
847	5.6	852	6.3	deformation
838	5.1			
762	6.6			
642	— <sup>a</sup>	636	44.1	$\sigma(\text{SO}_3)$

<sup>a</sup>Accurate absorbance could not be estimated because the sensitivity of the MCT detector was low in the wavenumber region below 655 cm<sup>-1</sup>.

<sup>b</sup>Intensities are represented as relative intensities, and those with relative intensity under 5 are omitted. All calculated wavenumbers are shown in Supporting Information (Table S4). The symbols  $\nu$  and  $\sigma$  represent stretching and bending vibrational modes, respectively.

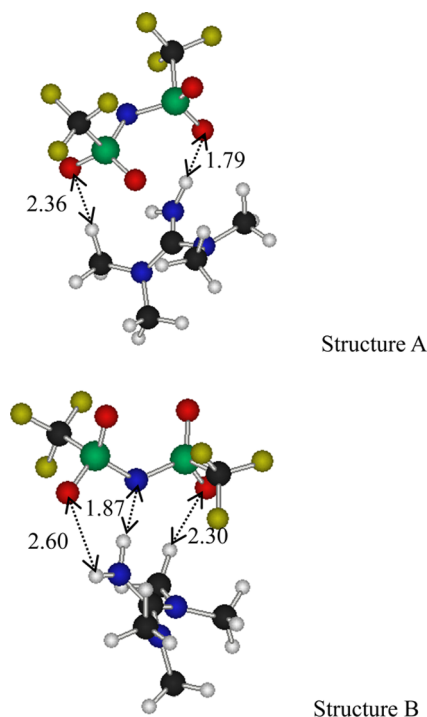


**Figure 8.** Most stable ion-pair structures of [H-TMG][Tf<sub>2</sub>N] calculated at the B3LYP/6-311++G(3df,3pd) level. The most and second-most stable structures are denoted by structure A and structure B, respectively. The hydrogen bonds are indicated by the distances in angstroms.

spectra of the parent acid and base molecules does not agree with the matrix-isolation spectrum of the vaporized PIL in the

**Table 3.** Observed and Calculated Wavenumbers of Neat [H-TMG][Tf<sub>2</sub>N] Liquid with Band Assignments

obs.		calc. of structure A <sup>b</sup>		
$\bar{\nu}$ (cm <sup>-1</sup> )	abs.	$\bar{\nu}$ (cm <sup>-1</sup> )	int. (km mol <sup>-1</sup> )	assignment
1651	16.5	1693	38.0	$\sigma(\text{HNH}) + \nu(\text{CN})$
1630	33.4	1638	90.4	$\nu_{\text{as}}(\text{NCN})$
1565	9.5	1597	33.4	$\nu_{\text{s}}(\text{NCN})$
1461	6.2			
1415	18.3	1451	15.2	$\sigma(\text{CH}_3)$
1360	17.3	1330	84.0	$\nu_{\text{as}}(\text{SO}_2)$
1350	19.4	1321	49.5	$\nu_{\text{as}}(\text{SO}_2)$
1328	9.6			
1238	15.3	1223	12.4	$\nu(\text{CF}_3) + \nu_{\text{s}}(\text{SO}_2)$
		1222	22.0	$\nu(\text{CF}_3) + \nu_{\text{as}}(\text{SNS})$
		1218	24.9	$\nu(\text{CF}_3) + \nu_{\text{as}}(\text{SNS})$
1215	38.8			
1210	100	1195	62.0	$\nu(\text{CF}_3)$
		1189	22.8	$\nu(\text{CF}_3)$
1202	88.3	1179	100	$\nu(\text{CF}_3) + \nu_{\text{s}}(\text{SO}_2)$
		1179	72.8	$\nu(\text{CF}_3) + \nu_{\text{s}}(\text{SO}_2)$
1146	31.4	1136	14.7	$\nu_{\text{s}}(\text{SO}_2)$
		1135	28.5	$\nu_{\text{s}}(\text{SO}_2)$
1140	47.9	1116	54.3	$\nu_{\text{s}}(\text{SO}_2)$
		1106	31.2	$\nu_{\text{s}}(\text{SO}_2)$
1073	9.0			
1064	29.4	1057	82.6	$\nu_{\text{as}}(\text{SNS})$
1056	15.3			
1042	4.3			
880	4.1	884	3.1	deformation
795	9.2	815	17.2	$\sigma(\text{NH}_2)$
744	4.5	783	10.9	$\sigma(\text{NH}_2) + \nu_{\text{s}}(\text{SNS})$
654	– <sup>a</sup>	659	29.5	$\sigma(\text{SNS})$

<sup>a</sup>Accurate absorbance could not be estimated because the sensitivity of the MCT detector was low in the wavenumber region below 655 cm<sup>-1</sup>.

<sup>b</sup>Intensities are represented as relative intensities, and those with relative intensity under 3 are omitted. All calculated wavenumbers are shown in Supporting Information (Table S5).

cases of both [H-TMG][Tf<sub>2</sub>N] and [H-TEA][Tf<sub>2</sub>N]. For example, the intense 857 cm<sup>-1</sup> band characteristic for HTf<sub>2</sub>N does not appear in Figures 5b and 6b. It should be mentioned here that the basicity is in increasing order of MIM < TEA < TMG as listed in Scheme 1. Additionally, we observed the temperature dependence of the matrix-isolation spectrum of [H-TEA][Tf<sub>2</sub>N]. The 857 cm<sup>-1</sup> band characteristic for HTf<sub>2</sub>N does not exist in Figure 6b recorded for the [H-TEA][Tf<sub>2</sub>N] matrix prepared at the vaporization temperature of 388 K, but it appears in Figure 6c where the matrix sample was prepared at 433 K. This observation means that at the elevated vaporization temperature of 433 K, neat [H-TEA][Tf<sub>2</sub>N] liquid vaporizes as the parent molecules in addition to the ion-pair form. We will discuss the temperature-dependent vaporization mechanism later.

**DFT Calculations.** We observed that three neat PILs, [H-TEA][OTf], [H-TMG][Tf<sub>2</sub>N] and [H-TEA][Tf<sub>2</sub>N], vaporize as the proton-transferred cation–anion form. We further assumed that the gaseous chemical species are of cation–anion 1:1 pairs in analogy with the gaseous components evaporated from aprotic ILs and then attempted to determine the ion-pair structures of PILs using DFT calculations. First, several stable ion-pair structures were explored at the B3LYP/6-31G\* level, and then the candidate structures were

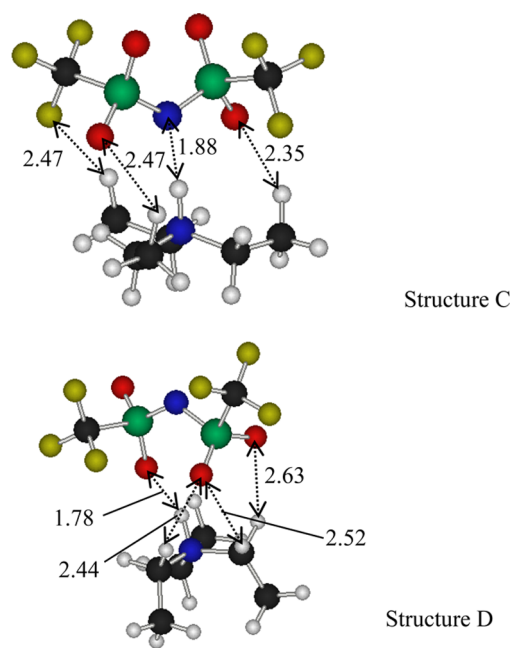


**Figure 9.** Most stable ion-pair structures of [H-TEA][Tf<sub>2</sub>N] calculated at the B3LYP/6-311++G(3df,3pd) level; the most and second-most stable structures are denoted by structure C and structure D, respectively. The hydrogen bonds are indicated by the distances in angstroms.

recalculated to estimate the optimized structures and theoretical IR spectra at the B3LYP/6-311++G(3df,3pd) level. For [H-TEA][OTf], the most stable ion-pair structure is estimated to lie ca. 46.5 kJ mol<sup>-1</sup> energetically below the second-most stable one, which is graphically shown in Figure 7. The moved proton is located 1.07 and 1.60 Å from the nitrogen atom of TEA and the oxygen atom on OTf, respectively, and all numerical values of the optimized nuclear coordinates are summarized in Supporting Information (Table S1). The ion pair is calculated to be located at 110.7 kJ mol<sup>-1</sup> below the parent molecules of TEA and OTf. Such energy difference implies that the ion pair does not dissociate into two parent molecules at the experimental vaporization temperature of 368 K. The simulated IR spectrum shown in Figure 3e satisfactorily reproduces the experimental matrix-isolation spectrum of Figure 3b, which suggests that neat [H-TEA][OTf] liquid is vaporized in a form of the optimized ion-pair structure illustrated in Figure 7. The spectral analysis based on the DFT calculation (Figure 3e) indicates that almost all the bands in Figure 3b originate from the vibrational modes of the [OTf] anion part. The measured and calculated wavenumbers, together with their vibrational assignments, are summarized in Table 2. As mentioned above, a discrepancy between the neat and matrix spectra is noticed in the asymmetrical SO<sub>3</sub> stretching region in the 1100–1400 cm<sup>-1</sup> region. The lower-wavenumber shift in the neat spectrum is explained by the free S=O bond in [OTf] shown in Figure 7 interacting with other ion pairs in the neat condition.

Figure 8 shows two ion-pair structures for [H-TMG][Tf<sub>2</sub>N], and their optimized nuclear coordinates are summarized in Supporting Information (Table S2). In the most stable structure A, the complex is formed through two stronger hydrogen bonds between the oxygen atom of Tf<sub>2</sub>N anion and the hydrogen atom of H-TMG cation, whereas in the second-most stable structure B, it is formed through three weaker

Table 4. Observed and Calculated Wavenumbers of Neat [H-TEA][Tf<sub>2</sub>N] Liquid with Band Assignments

obs.		calc. of structure D <sup>b</sup>		
$\tilde{\nu}$ (cm <sup>-1</sup> )	abs.	$\tilde{\nu}$ (cm <sup>-1</sup> )	int. (km mol <sup>-1</sup> )	assignment
1604	3.6			
1479	5.1			
1462	5.1	1438	7.4	$\sigma(\text{NH}) + \sigma(\text{CH}_2) + \sigma(\text{CH}_3)$
		1383	5.7	$\sigma(\text{CH}_2)$
1388	19.0			$\nu_{\text{as}}(\text{SO}_2)$ for structure C
1362	49.2	1343	99.4	$\nu_{\text{as}}(\text{SO}_2)$
		1334	9.2	$\sigma(\text{CH}_2)$
1343	19.0	1314	28.2	deformation + $\nu_{\text{as}}(\text{SO}_2)$
1332	9.5	1308	29.3	deformation + $\nu_{\text{as}}(\text{SO}_2)$
1298	9.1			
1279	4.2			
1243	23.6	1225	14.5	$\nu(\text{CF}_3) + \nu_s(\text{SO}_2)$
1233	12.6	1219	51.3	$\nu(\text{CF}_3) + \nu_{\text{as}}(\text{SNS})$
		1198	7.1	CH <sub>3</sub> rocking + $\sigma(\text{CH}_2) + \nu(\text{CF}_3)$
1223	29.5	1196	25.1	$\nu(\text{CF}_3)$
1218	100	1193	100	$\nu(\text{CF}_3)$
1213	75.2			
1195	67.6	1177	72.4	$\nu(\text{CF}_3)$
		1175	12.4	$\nu(\text{CF}_3) + \text{CH}_3$ rocking
1179	15.6	1166	47.6	$\nu(\text{CF}_3)$
1140	48.8	1120	96.8	$\nu_s(\text{SO}_2) + \nu_{\text{as}}(\text{SNS})$
		1117	33.0	$\nu_s(\text{SO}_2) + \nu_{\text{as}}(\text{SNS})$
		1079	5.3	CH <sub>3</sub> rocking
1073	28.7	1053	67.4	$\nu_{\text{as}}(\text{SNS})$
1047	9.8	1039	5.5	$\nu(\text{CN})$
1039	16.5			$\nu_{\text{as}}(\text{SNS})$ for structure C
794	7.0	792	5.6	$\nu_s(\text{SNS})$
747	4.8			
658	12.1	665	27.8	$\sigma(\text{SNS})$
625	– <sup>a</sup>	604	9.7	$\sigma(\text{SO}_2\text{N}) + \sigma(\text{CCN})$

<sup>a</sup>Accurate absorbance could not be estimated because the sensitivity of the MCT detector was low in the wavenumber region below 655 cm<sup>-1</sup>.

<sup>b</sup>Intensities are represented as relative intensities, and those with relative intensity under 5 are omitted. All calculated wavenumbers are shown in Supporting Information (Table S6).

hydrogen bonds with an additional bond between the nitrogen atom of the anion and the hydrogen atom of the cation. Structure A is estimated to be 11.0 kJ mol<sup>-1</sup> more stable than structure B, and the estimated energy gap indicates that the gaseous ion pair evaporated at 428 K is dominantly in a form of structure A. The simulated IR spectrum shown in Figure 5e satisfactorily reproduces the experimental matrix-isolation spectrum of Figure 5b, which suggests that the PIL of [H-TMG][Tf<sub>2</sub>N] is vaporized mainly in a form of the most stable ion pair. Considering the S–N–S symmetrical stretching vibration region of 1100 and 900 cm<sup>-1</sup>, the band simulation of structure A having a free nitrogen atom of Tf<sub>2</sub>N part seems to reproduce the experiment better than that of structure B having a hydrogen-bonded nitrogen atom of the Tf<sub>2</sub>N part. Both of the energetics and spectral patterns indicate that the gaseous species of [H-TMG][Tf<sub>2</sub>N] is of the ion pair of structure A. The measured and calculated wavenumbers are summarized in Table 3.

Figure 9 shows two candidates for gaseous species of [H-TEA][Tf<sub>2</sub>N], where structure C is calculated to be slightly more stable than structure D (by 2.0 kJ mol<sup>-1</sup>), and their optimized geometries are summarized in Supporting Information (Table S3). The estimated energy difference indicates that both structures coexist in the gas phase at the vaporization temperature of 408 K ( $RT \sim 3$  kJ mol<sup>-1</sup>). Their theoretical

spectra are also shown in Figure 6f,g, which supports an assignment of the experimental matrix-isolation spectrum (Figure 6b) to structure D (Figure 6g) rather than structure C (Figure 6f). For instance, the signature 1073 and 1362 cm<sup>-1</sup> bands of the spectrum in Figure 6b correspond with the 1053 and 1343 bands calculated for structure D (Figure 6g) rather than the 1013 and 1387 bands for structure C (Figure 6f). Most of the observed intense bands are consistent with the bands of structure D, but the weak bands around 1040 and 1390 cm<sup>-1</sup> may be those due to structure C. We tentatively conclude that [H-TEA][Tf<sub>2</sub>N] evaporates in ion pairs mainly of structure D, possibly with the minor contribution of structure C. The mismatch between observation and simulation remains unclear at the present stage, though the DFT calculation accuracy at the B3LYP/6-311++G(3df,3pd) level might not be sufficient. The measured and calculated wavenumbers are summarized in Table 4.

**Vaporization Mechanism.** Table 1 summarizes the detected gaseous species evaporated from protic ILs studied in the present study. Parent acid and base molecules tend to be released from the PILs of lower  $\Delta pK_a$  values, whereas ion pairs are detected as vaporization components obtained from the PILs of higher  $\Delta pK_a$  values. The phenomena will be explained by thermodynamic equilibrium between acid–base and anion–cation systems in the liquid phase. Lower  $\Delta pK_a$  PILs are

synthesized by combining a weaker acid and a weaker base, where a certain concentration of parent acid and base molecules are expected to coexist in neat protic ILs at room temperature. Then, the acid and base molecules are evaporable without heating neat PIL, which corresponds to examples of [H-MIM][AcO] and [H-TEA][AcO]. Higher  $\Delta pK_a$  PILs prepared by a stronger acid and a stronger base and the equilibrium between acid–base and anion–cation pairs shifts to the anion–cation pair side in the liquid, where less concentration of parent molecules exist in the liquid at room temperature. With increasing temperature, the acid and base concentration increases in the liquid and then they are vaporized at a temperature lower than that of ion-pair vaporization, which corresponds to an example of [H-MIM][Tf<sub>2</sub>N]. Much higher  $\Delta pK_a$  PILs are prepared by combining a strong acid and a strong base, where the concentration of deprotonated acid and protonated base dominates in the liquid. The parent acid and base do not exist in the liquid at the temperature of the PIL vaporization. As a result, the corresponding acid and base vanishingly exist in the gaseous component, and then the PILs with high  $\Delta pK_a$  behave like aprotic ILs vaporizing to be ion pairs. This hypothesis may be confirmed by the temperature-dependent experimental result for [H-TEA][Tf<sub>2</sub>N] as shown in Figure 6, where the parent molecules were observed at higher temperature, 433 K. This indicates that the population of the parent molecules may be negligible in the liquid at 388 K but increases with temperature to the extent that the detectable acid and base molecules are evaporated from the neat PIL liquid at 433 K.

## CONCLUSION

Several kinds of PILs with various  $\Delta pK_a$  values synthesized by combinations of three acids and three bases were investigated by matrix-isolation IR spectroscopy with the aid of DFT calculations. When matrix spectra of the PILs are compared with those of the corresponding parent acid and base molecules, the three PILs of [H-MIM][AcO], [H-TEA][AcO], and [H-MIM][Tf<sub>2</sub>N] are evaporated to be the corresponding parent acids and bases while [H-TEA][OTf], [H-TEA][Tf<sub>2</sub>N], and [H-TMG][Tf<sub>2</sub>N] exist to form ion-pair structures in the gas phases. This classification is related to their  $\Delta pK_a$  values. While the lower  $\Delta pK_a$  PILs vaporize to become the parent Brønsted acids and bases as well as the previous suggestions,<sup>3</sup> the PILs with higher  $\Delta pK_a$  form an ion-pair structure in the gas phase similar to that of the well-known vaporization of aprotic ILs.

## ASSOCIATED CONTENT

### Supporting Information

Full description of calculated results. This material is available free of charge via the Internet at <http://pubs.acs.org>.

## AUTHOR INFORMATION

### Corresponding Author

\*

### Notes

The authors declare no competing financial interest.

## ACKNOWLEDGMENTS

This work was financially supported in part by Grant-in-Aid for Scientific Research 24750013 and 24350004 from the Ministry of Education, Culture, Sports, Science and Technology, Japan.

## REFERENCES

- (1) Earle, M. J.; Esperanca, J.; Gilea, M. A.; Lopes, J. N. C.; Rebelo, L. P. N.; Magee, J. W.; Seddon, K. R.; Widegren, J. A. Distillation and Volatility of Ionic Liquids. *Nature (London, U.K.)* **2006**, *439*, 831–834.
- (2) Gross, J. H. Molecular Ions of Ionic Liquids in the Gas Phase. *J. Am. Soc. Mass Spectrom.* **2008**, *19*, 1347–1352.
- (3) Leal, J. P.; Esperanca, J.; da Piedade, M. E.M.; Lopes, J. N. C.; Rebelo, L. P. N.; Seddon, K. R. The Nature of Ionic Liquids in the Gas Phase. *J. Phys. Chem. A* **2007**, *111*, 6176–6182.
- (4) Armstrong, J. P.; Hurst, C.; Jones, R. G.; Licence, P.; Lovelock, K. R. J.; Satterley, C. J.; Villar-Garcia, I. J. Vaporisation of Ionic Liquids. *Phys. Chem. Chem. Phys.* **2007**, *9*, 982–990.
- (5) Deyko, A.; Lovelock, K. R. J.; Licence, P.; Jones, R. G. The vapour of imidazolium-based ionic liquids: A mass spectrometry study. *Phys. Chem. Chem. Phys.* **2011**, *13*, 16841–16850.
- (6) Neto, B. A. D.; Meurer, E. C.; Galaverna, R.; Bythell, B. J.; Dupont, J.; Cooks, R. G.; Eberlin, M. N. Vapors from Ionic Liquids: Reconciling Simulations with Mass Spectrometric Data. *J. Phys. Chem. Lett.* **2012**, *3*, 3435–3441.
- (7) Akai, N.; Kawai, A.; Shibuya, K. First observation of the matrix-isolated FTIR spectrum of vaporized ionic liquid: An example of *mimTFSI*, 1-Ethyl-3-methylimidazolium bis-(trifluoromethanesulfonyl)imide. *Chem. Lett.* **2008**, *37*, 256–257.
- (8) Akai, N.; Parazs, D.; Kawai, A.; Shibuya, K. Cryogenic neon matrix-isolation FTIR spectroscopy of evaporated ionic liquids: Geometrical structure of cation–anion 1:1 pair in the gas phase. *J. Phys. Chem. B* **2009**, *113*, 4756–4762.
- (9) Strasser, D.; Goulay, F.; Belau, L.; Kostko, O.; Koh, C.; Chambreau, S. D.; Vaghjani, G. L.; Ahmed, M.; Leone, S. R. Tunable Wavelength Soft Photoionization of Ionic Liquid Vapors. *J. Phys. Chem. A* **2010**, *114*, 879–883.
- (10) Chambreau, S. D.; Vaghjani, G. L.; To, A.; Koh, C.; Strasser, D.; Kostko, O.; Leone, S. R. Heats of Vaporization of Room Temperature Ionic Liquids by Tunable Vacuum Ultraviolet Photoionization. *J. Phys. Chem. B* **2010**, *114*, 1361–1367.
- (11) Wang, C.; Luo, H.; Li, H.; Dai, S. Direct UV-spectroscopic measurement of selected ionic-liquid vapors. *Phys. Chem. Chem. Phys.* **2010**, *12*, 7264–7250.
- (12) Akai, N.; Kawai, A.; Shibuya, K. Ion-Pair Structure of Vaporized Ionic Liquid Studied by Matrix-Isolation FTIR Spectroscopy with DFT Calculation: A Case of 1-Ethyl-3-methylimidazolium Trifluoromethanesulfonate. *J. Phys. Chem. A* **2010**, *114*, 12662–12666.
- (13) Ogura, T.; Akai, N.; Kawai, A.; Shibuya, K. Gas phase electronic absorption spectroscopy of room temperature ionic liquids: *N*-Ethyl-3-methylpyridinium or 1-butyl-3-methylimidazolium cation with bis-(trifluoromethylsulfonyl)amido anion. *Chem. Phys. Lett.* **2013**, *555*, 110–114.
- (14) Dong, K.; Zhao, L.; Wang, Q.; Song, Y.; Zhang, S. Are ionic liquids pairwise in gas phase? A cluster approach and in situ IR study. *Phys. Chem. Chem. Phys.* **2013**, *15*, 6034–6040.
- (15) Obi, E. I.; Leavitt, C. M.; Raston, P. L.; Moradi, C. P.; Flynn, S. D.; Vaghjani, G. L.; Boatz, J. A.; Chambreau, S. D.; Doublerly, G. E. Helium Nanodroplet Isolation and Infrared Spectroscopy of the Isolated Ion-Pair 1-Ethyl-3-methylimidazolium bis(trifluoromethylsulfonyl)imide. *J. Phys. Chem. A* **2013**, *117*, 9047–9056.
- (16) Kelkar, M. S.; Maginn, E. J. Calculating the Enthalpy of Vaporization for Ionic Liquid Clusters. *J. Phys. Chem. B* **2007**, *111*, 9424–9427.
- (17) Rai, N.; Maginn, E. J. Vapor–Liquid Coexistence and Critical Behavior of Ionic Liquids via Molecular Simulations. *J. Phys. Chem. Lett.* **2011**, *2*, 1439–1443.
- (18) Chaban, V. V.; Prezhdo, O. V. Ionic Vapor: What Does It Consist Of? *J. Phys. Chem. Lett.* **2012**, *3*, 1657–1662.
- (19) Malberg, F.; Pensado, A. S.; Kirchner, B. The bulk and the gas phase of 1-ethylimidazolium ethylsulfate: Dispersion interaction makes the difference. *Phys. Chem. Chem. Phys.* **2012**, *14*, 12079–12082.
- (20) Paulechka, Y. U.; Zaitsau, D. H.; Kabo, G. J.; Strechan, A. A. Vapor pressure and thermal stability of ionic liquid 1-butyl-3-

methylimidazolium Bis(trifluoromethylsulfonyl)amide. *Thermochim. Acta* **2005**, *439*, 158–160.

(21) Santos, L. M. N. B. F.; Lopes, J. N. C.; Coutinho, J. A. P.; Esperança, J. M. S. S.; Gomes, L. R.; Marrucho, I. M.; Rebelo, L. P. N. Ionic Liquids: First Direct Determination of their Cohesive Energy. *J. Am. Chem. Soc.* **2007**, *129*, 284–285.

(22) Esperança, J. M. S. S.; Lopes, J. N. C.; Tariq, M.; Santos, L. M. N. B. F.; Magee, J. W.; Rebelo, L. P. N. Volatility of Aprotic Ionic Liquids – A Review. *J. Chem. Eng. Data* **2010**, *55*, 3–12.

(23) Lovelock, K. R. J.; Deyko, A.; Corfield, J.; Gooden, P. N.; Licence, P.; Jones, R. G. Vaporisation of a Dicationic Ionic Liquid. *ChemPhysChem* **2009**, *10*, 337–340.

(24) Deyko, A.; Lovelock, K. R. J.; Corfield, J.; Taylor, A. W.; Gooden, P. N.; Villar-Garcia, I. J.; Licence, P.; Jones, R. G.; Krasovskiy, V. G.; Chernikova, E. A.; Kustov, L. M. Measuring and predicting  $\Delta_{\text{vap}}H_{298}$  values of ionic liquids. *Phys. Chem. Chem. Phys.* **2009**, *11*, 8544–8555.

(25) Vitorino, J.; Leal, J. P.; Licence, P.; Lovelock, K. R. J.; Gooden, P. N.; da Piedade, M. E. M.; Shimizu, K.; Rebelo, L. P. N.; Lopes, J. N. C. Vaporisation of a Dicationic Ionic Liquid Revisited. *ChemPhysChem* **2010**, *11*, 3637–3677.

(26) Berg, R. W.; Lopes, J. N. C.; Ferreira, R.; Rebelo, L. P. N.; Seddon, K. R.; Tomaszowska, A. A. Raman Spectroscopic Study of the Vapor Phase of 1-Methylimidazolium Ethanoate, a Protic Ionic Liquid. *J. Phys. Chem. A* **2010**, *114*, 10834–10841.

(27) Berg, R. W.; Riisager, A.; Fehrmann, R. Formation of an Ion-Pair Molecule with a Single  $\text{NH}^+\cdots\text{Cl}^-$  Hydrogen Bond: Raman Spectra of 1,1,3,3-Tetramethylguanidinium Chloride in the Solid State, in Solution, and in the Vapor Phase. *J. Phys. Chem. A* **2008**, *112*, 8585–8592.

(28) Berg, R. W.; Riisager, A.; Van Buu, O. N.; Kristensen, S. B.; Fehrmann, R.; Harris, P.; Brunetti, A. C. X-ray Crystal Structure, Raman Spectroscopy, and Ab Initio Density Functional Theory Calculations on 1,1,3,3-Tetramethylguanidinium Bromide. *J. Phys. Chem. A* **2010**, *114*, 13175–13181.

(29) Vitorino, J.; Leal, J. P.; da Piedade, M. E. M.; Lopes, J. N. C.; Esperança, J. M. S. S.; Rebelo, L. P. N. The Nature of Protic Ionic Liquids in the Gas Phase Revisited: Fourier Transfer Ion Cyclotron Resonance Mass Spectrometry Study of 1,1,3,3-Tetramethylguanidinium Chloride. *J. Phys. Chem. B* **2010**, *114*, 8905–8909.

(30) Emelyanenko, V. N.; Varevkin, S. P.; Heintz, A.; Voss, K.; Schulz, A. Imidazolium-Based Ionic Liquids. 1-Methyl Imidazolium Nitrate: Thermochemical Measurements and Ab Initio Calculations. *J. Phys. Chem. B* **2009**, *113*, 9871–9876.

(31) Zhu, X.; Wang, Y.; Li, H. Do all the protic ionic liquids exist as molecular aggregates in the gas phase? *Phys. Chem. Chem. Phys.* **2011**, *13*, 17445–17448.

(32) Vitorino, J.; Bernardes, C. E. S.; da Piedade, M. E. M. A general strategy for the experimental study of the thermochemistry of protic ionic liquids: Enthalpy of formation and vaporization of 1-methylimidazolium ethanoate. *Phys. Chem. Chem. Phys.* **2012**, *14*, 4440–4446.

(33) Greaves, T. L.; Drummond, C. J. Protic Ionic Liquids: Properties and Applications. *Chem. Rev. (Washington, DC, U.S.)* **2008**, *108*, 206–237.

(34) Stoimenovski, J.; Izgorodina, E.; MacFarlane, D. R. Ionicity and proton transfer in protic ionic liquids. *Phys. Chem. Chem. Phys.* **2010**, *12*, 10341–10347.

(35) Miran, M. S.; Kinoshita, H.; Yasuda, T.; Susan, Md. A. B. H.; Watanabe, M. Physicochemical properties determined by  $\Delta pK_a$  for protic ionic liquids based on an organic super-strong base with various Brønsted acids. *Phys. Chem. Chem. Phys.* **2012**, *14*, 5178–5186.

(36) Frisch, M. J.; Trucks, G. W.; Schlegel, H. B.; Scuseria, G. E.; Robb, M. A.; Cheeseman, J. R.; Scalmani, G.; Barone, V.; Mennucci, B.; Petersson, G. A. et al. *Gaussian 09*, revision C.1; Gaussian, Inc.: Wallingford, CT, 2009.